BJPS

Brazilian Journal of Pharmaceutical Sciences

http://dx.doi.org/10.1590/s2175-97902023e22459

Article

Selective photodynamic effects on cervical adenocarcinoma cells provided by F127 Pluronic®-based micelles modulating hypericin delivery

Kayane Harumi Mashiba[1,†], Lucimara Rofrigues Carobeli[1,†], Maria Vítoria Felipe de Souza[1], Lyvia Eloiza de Freitas Meirelles[1], Natália Lourenço Mari[1], Gabriel Batista César[2], Renato Sonchini Gonçalves[2], Wilker Caetano[2], Edilson Damke[1], Vânia Ramos Sela da Silva[1], Gabrielle Marconi Zago Ferreira Damke[1], Marcia Edilaine Lopes Consolaro[1,*]

[1]Department of Clinical Analysis and Biomedicine, Universidade Estadual de Maringá, Maringá, Paraná, Brazil, [2]Department of Chemistry, Universidade Estadual de Maringá, Maringá, Paraná, Brazil

[†]These authors contributed equally to this work.

Cervical cancer is a leading cause of death among women. The endocervical adenocarcinoma (ECA) represents an aggressive and metastatic type of cancer with no effective treatment options currently available. We evaluated the antitumoral and anti-migratory effects of hypericin (HYP) encapsulated on Pluronic F127 (F127/HYP) photodynamic therapy (PDT) against a human cell line derived from invasive cervical adenocarcinoma (HeLa) compared to a human epithelial cell line (HaCaT). The phototoxicity and cytotoxicity of F127/HYP were evaluated by the following assays: colorimetric assay, MTT, cellular morphological changes by microscopy and long-term cytotoxicity by clonogenic assay. In addition, we performed fluorescence microscopy to analyze cell uptake and subcellular distribution of F127/HYP, cell death pathway and reactive oxygen species (ROS) production. The PDT mechanism was determined with sodium azide and D-mannitol and cell migration by wound-healing assay. The treatment with F127/HYP promoted a phototoxic result in the HeLa cells in a dose-dependent and selective form. Internalization of F127/HYP was observed mainly in the mitochondria, causing cell death by necrosis and ROS production especially by the type II PDT mechanism. Furthermore, F127/HYP reduced the long-term proliferation and migration capacity of HeLa cells. Overall, our results indicate a potentially application of F127/HYP micelles as a novel approach for PDT with HYP delivery to more specifically treat ECA.

Keywords: Photochemotherapy, Endocervical adenocarcinoma, HeLa cells, Hypericin, Pluronic F127, Drug delivery systems.

INTRODUCTION

Cervical cancer is currently one of the most common types of cancer in women worldwide with an estimated 604,000 cases and 342,000 deaths worldwide in 2020 (Sung *et al*., 2021). The most prevalent cervical malignancy - invasive squamous cell carcinoma (SCC) - is almost always caused by human papillomavirus (HPV) infection being HPV-16 the most prevalent type followed by HPV-18. The implementation of national screening and vaccination programs in most developed countries has reduced its incidence over the last few decades (Kurman *et al*., 2014). In contrast, invasive endocervical

***Correspondence:** M. E. L. Consolaro. Departmento de Análises Clínicas e Biomedicina. Universidade Estadual de Maringá. Av. Colombo, 5790. 87020-900, Maringá, Paraná, Brasil. E-mail: melconsolaro@gmail.com. ORCID: https://orcid.org/0000-0001-9102-4865 | L. R. Carobeli - ORCID: https://orcid.org/0000-0003-3066-4708

adenocarcinoma (ECA) is less common, accounting for about 25% of cervical malignancies; however, its prevalence is rising, particularly among young women in developed countries, even in those with functional screening programs (Loureiro, Oliva, 2014).

International endocervical adenocarcinoma criteria and classification (IECC) classifies ECA into two major subtypes: HPV-associated and non-HPV-associated. This classification incorporates etiology, distinctive morphologic patterns and clinical finding (Stolnicu *et al*., 2019). Most fo the ECAs are associated to HPV-18, -16, and -45 in equal prevalence, although some epidemiologic studies suggest that the HPV-18 type is the most common (Loureiro, Oliva, 2014). Compared to SCC, ECA is a heterogeneous group of tumors that present a poorer prognosis although there are no differences in the treatment strategy between them and between the different types of ECA (Yokoi *et al*., 2017). Additionally, several previous studies suggested that ECA is more aggressive than SCC (Paik *et al*., 2020). These data underscore the need for different treatment strategies for ECA patients.

Photodynamic therapy (PDT) has emerged as an effective therapeutic alternative to treat oncological diseases. The main elements of PDT are a photoactive drug (PS), light at an appropriate wavelength and molecular oxygen (Robertson, Evans, Abrahamse, 2009). Light excites the PS to its triplet state, interacting with the oxygen present in the tissue to produce reactive oxygen species (ROS) via a type I or type II mechanism. This interaction results in the production of free radicals (Fuchs, Thiele, 1998) or singlet oxygen ($^1O_2$) (Ochsner, 1997), respectively. PDT is an attractive modality for cancer treatment because the PS, light and oxygen separately do not present any toxic effects to the body, unlike chemotherapy which induces systemic toxicity and radiotherapy which damages neighboring normal tissues (Agostinis *et al*., 2011). A number of PSs are already in clinical use or in clinical trials to treat cancer patients, including Hypericin (HYP), a naphthodianthrone compound widely used in clinical modalities not associated to light excitation (Hudson, Lopez-Bazzocchi, Towers, 1991). HYP can be obtained by extraction from leaves of *Hypericum perforatum* species or through synthetic processes (Falk, Schoppel 1992). After illumination, this compound leads to cytotoxic effects resulting in cell death by necrosis and/or apoptosis in different cancer cell lines (Chung *et al*., 1994). These properties, added to low toxicity in the dark, specificity for tumors and a high clearance rate in the body, indicates that HYP is a promising PS for PDT against cancer (Karioti, Bilia, 2010). However, as with most PS, HYP presents high hydrophobicity and form aggregates in aqueous media and body fluids (Kubin *et al*., 2008). The hydrophobic interactions can affect their photophysical (reducing $^1O_2$ generation), chemical (reduced solubility) and biological effects. Hence, it is imperative to use drug delivery systems (DDSs) to overcome this shortcoming (Tatischeff, Alfsen, 2011).

Pluronic F127 is an amphiphilic triblock copolymer composed of poly (ethylene oxide) (PEO) and poly (propylene oxide) (PPO), PEO-x-PPO-y-PEO-x). Amphiphilic block copolymers self-assemble spontaneously in aqueous environments into polymeric nanostructures known as micelles and for this reason they have been commonly used to solubilize hydrophobic drugs in DDS (Gregoriou *et al*., 2021). As shown in Scheme 1, the PEO block of F127 is hydrophilic and forms the outside layer of the nanoparticle while the PPO block is hydrophobic and composes the inner core. The hydrophobic core serves as a reservoir in which the hydrophobic drug molecule can be incorporated and protected from inactivation in biological media so it can be delivered effectively to the malignancy while the hydrophilic shell promotes the delivery of the drug to target cells (Imran, Shah, Shafi, 2018). Pluronic F127 has attracted a lot of attention in drug delivery because of its low toxicity in the body and the ability to nanoencapsulate hydrophobic agents. Additionally, Pluronic F127 improves pro-apoptotic signaling, sensitizing tumor cells and increasing their susceptibility to the actions of anti-cancer drugs (Imran, Shah, Shafi, 2018). Our most recent study in this field showed the efficiency and selectivity of HYP-loaded pluronic F127 micelles for PDT against triple-negative breast cancer (MDA-MB-231) (de Souza *et al*., 2022). However, to the best of our knowledge, no study to date has evaluated the activity of HYP encapsulated with Pluronic F127 (F127/HYP) against ECA.

To better understand the activity of F127/HYP and explore its possible capability as a new therapeutic candidate for ECA treatment, we evaluated the effects of F127/HYP PDT against the human cell line derived from invasive adenocarcinoma cervical (HeLa) compared to a nontumorigenic human epithelial cell line (HaCaT). The aims of this study were to investigate the effects of F127/HYP on HeLa and HaCaT cells with respect to (i) cell cytotoxicity and phototoxicity, cellular uptake and subcellular distribution; (ii) cell death pathway and cellular oxidative stress; and (iii) migration. Our results demonstrated that F127/HYP has a selective phototoxic effect inducing necrosis in HeLa cells, but not in HaCaT cells. Additionally, F127/HYP PDT induced ROS generation mainly via the type II mechanism of PDT and inhibited cancer cell migration. F127/HYP PDT presented a high and selective antitumoral effect on ECA cells immortalized by HPV-18, indicating its potential to be a powerful candidate in developing therapeutic agents against ECA.

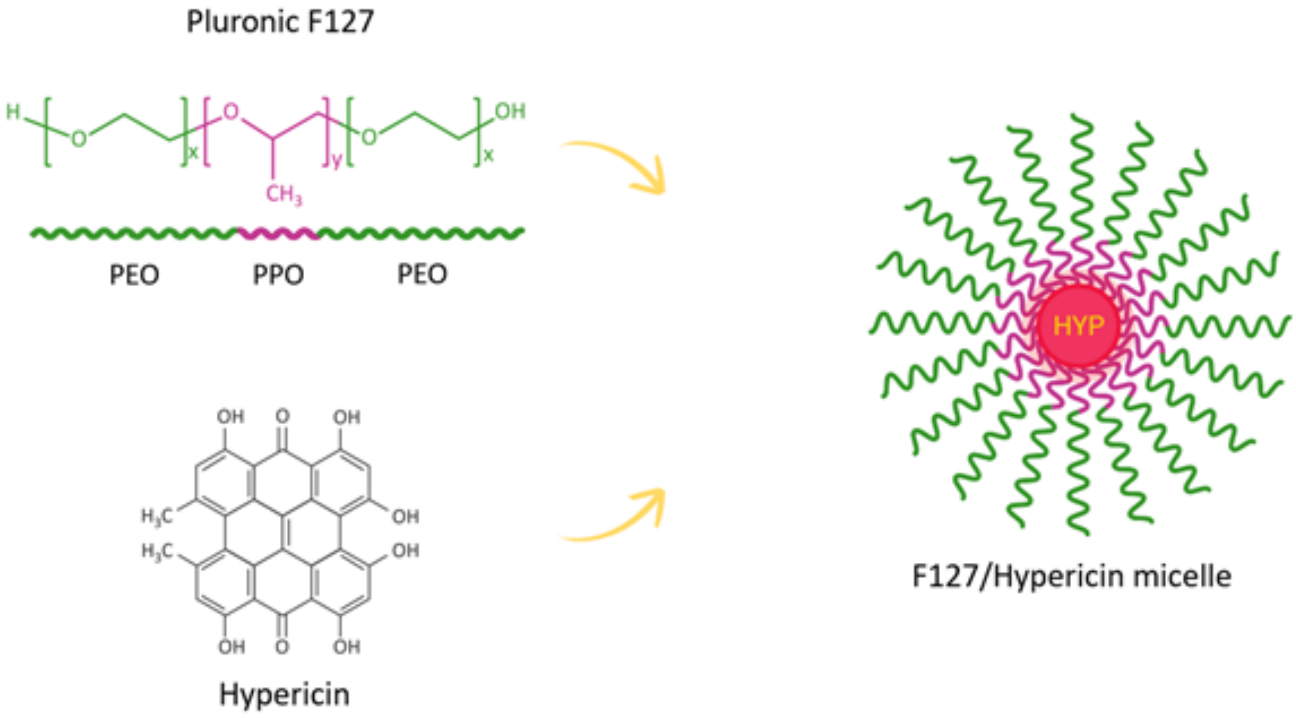

SCHEME 1 - Structure of F127 pluronic and hypericin micelles. The hydrophilic regions consisting of ethylene oxide (PEO) are represented in green and form the outer face of the nanoparticle. The hydrophobic regions composed of propylene oxide (PPO) are represented in pink and form the inner core that houses hypericin, also hydrophobic, extracted from *Hypericum perforatum* or obtained by synthetic processes.

MATERIAL AND METHODS

Photosensitizer and LED Illumination

HYP was synthesized and characterized by the Research Nucleus in Photodynamic Systems and Nanomedicine (NUPESF), Chemistry Department, State University of Maringa/PR/Brazil, according to a previous study (Gonçalves *et al*., 2017). Formulations containing HYP (1,3,4,6,8,13-hexahidroxi-10,11-dimetilfenantro [1,10,9,8-opqra] perileno-7,14-diona, C30H16O8, 98% purity) in nanostructures of Pluronic® F127 were prepared following the solid dispersion method (Zhang, Jackson, Burt, 1996). The formulation was freeze-dried

and prior to each treatment was rehydrated with sterile phosphate-buffered saline (PBS) (250 µmol/L F127/100 µmol/L HYP). Preparation and quality control of F127/HYP formulation were previously determined by our research group and have been published by de Souza *et al*. (2022).

A light source device with 66 light-emitting diodes (LED) units emitting white light at 6.3 J/cm^2 in a wavelength range from 450 to 750 nm was kindly supplied by the NUPESF, to illuminate the entire area of the cell culture plates. To prevent light interference, all irradiation tests were performed in absence of light.

Cell lines and culture conditions

The human cell line derived from invasive cervical adenocarcinoma, HeLa (integrated HPV-18) and the spontaneously immortalized human epithelial cell line HaCaT (non-tumorigenic cells) were kindly donated by Dr. Luisa L. Villa, School of Medicine, University of São Paulo/SP/Brazil and Dr. Silvya S. Maria-Engler, Faculty of Pharmaceutical Sciences, University of São Paulo/SP/Brazil. The cell lines were maintained in a culture flask in Dulbecco's modified Eagle medium (DMEM) supplemented with 10% fetal bovine serum (FBS), 1% penicillin/streptomycin, and 1% amphotericin B solution, at 37 °C in a humidified atmosphere with 5% CO_2.

Cytotoxicity and phototoxicity

Cell viability was assessed by MTT [3-(4,5-dimethylthiazol-2-yl)-2,5-diphenyltetrazolium bromide] assay (Kumar *et al*., 2018). HeLa and HaCaT cell lines were seeded in 96-well tissue culture plates with 200 µL/well at a density of 2.5 × 10^5 cells/mL. The cells were allowed to attach overnight (24 h) at 37 °C in a humidified atmosphere with 5% CO_2. After, the cells were treated with F127/HYP at different concentrations (0.4, 0.6, 0.8, 1.0, 1.2, 1.4, 1.6, 1.8, 2.0, 2.2, 2.4, 2.6, 2.8, 3.0 and 3.2 µmol/L of HYP) for 30 min in the absence of light. To evaluate the phototoxicity, after incubation with the same concentrations of F127/HYP for 30 min in the absence of light, the cells were exposed to a light source for 15 min. Next, they were incubated again in the dark for 30 min. Cells exposed only to DMEM or F127 (1.94 µmol/L) were considered as untreated controls in all assays.

Following, 50 µL of MTT solution in a final concentration of 5 mg/mL was added to each well and the plates were incubated in absence of light at 37 °C for 4h. After incubation, 150 µL of DMSO was added to solubilize the formazan resulting from the reaction. The absorbance was measured at 570 nm using a microplate reader. (Loccus, Cotia, SP, Brazil). From the data obtained, the concentrations that inhibited cell growth by 30% (IC_{30}), 50% (IC_{50}) and 90% (IC_{90}) compared to the untreated cells (NT) were calculated. Non-linear regression analysis was performed using GraphPad Prism 6.0 (GraphPad Software, San Diego, USA).

Cell morphology

HeLa cell line was seeded in a 24-well tissue culture plate with 500 µL/well at a density of 1.5 × 10^5 cells/mL. The cells were allowed to attach overnight in the incubator and then were treated with 0.4, 1.8 and 3.2 µmol/L of F127/HYP for 30 min in the dark, illuminated for 15 min and incubated in the absence of light for 30 min. The cells exposed only to DMEM were used as NT. The growth and morphology of the cells were observed in an inverted microscope (EVOS® FL, Life Technologies, USA).

Clonogenic assay

In order to establish the long-term cytotoxicity effects of F127/HYP PDT, HeLa cells were seeded in a 6-well tissue culture plate with 2 mL/well at a density of 600 cells/well. After 24h, they were treated with IC_{30} and IC_{50} values of F127/HYP for 30 min in the absence of light, illuminated for 15 min and incubated in the absence of light for 30 min. Next, the plates were incubated in ideal conditions for 7 or 14 days (the medium was changed after 7 days for the cells incubated for 14 days). The cells treated with DMEM without FBS were used as NT. The colonies formed were stained with crystal violet solution after fixation with methanol and counted manually (Franken *et al*., 2006).

Cellular uptake

HeLa and HaCaT cell lines were seeded in a 24-well tissue culture plate with 500 µL/well at a density of 1.5 × 10^5 cells/mL. The cells were allowed to attach overnight in the incubator, then was added 1 µmol/L HYP/F127 and incubated for 30 min. To display the fluorescence emitted by HYP inside the cell, an inverted fluorescence microscope with an RFP (red) filter (EVOS® FL, Life Technologies, USA) was used.

Subcellular distribution

HeLa cell line was seeded in a 24-well tissue culture plate with 500 µL/well at a density of 1.5 ×10^5 cells/mL and the cells were allowed to attach overnight in the incubator. After, the cells were incubated for 15 min with subcellular organelle probes specific for mitochondria (MitoTracker® excitation: 490 nm and emission: 516 nm) and nucleus (NucBlue® Live ReadyProbes® excitation: 360 nm and emission: 460 nm) and for 30 min with F127/HYP (5 µmol/L). To display the fluorescence emitted by F127/HYP and the stained cell structures, an inverted fluorescence microscope with DAPI (blue), RFP (red) and GFP (green) filters (EVOS® FL, Life Technologies, USA) was used.

Cell Death Pathways by annexin V-FITC/propidium iodide (PI)

HeLa cell line was seeded in 24-well tissue culture plates with 500 µL/well at a density of 2.5×10^5. The cells were allowed to attach overnight at 37 °C in a humidified atmosphere with 5% CO_2 and then treated with IC_{50} value of F127/HYP for 30 min in the absence of light, illuminated for 15 min and incubated in the absence of light for 30 min. After treatment, cells were washed with PBS and binding buffer (10 mM of HEPES Invitrogen, USA, pH 7.5, containing 140 mM of NaCl and 2.5 mM of $CaCl_2$, Synth, Brazil) and stained with 1 µg/mL of FITC-conjugated annexin-V (Invitrogen, USA) for 15 min and 40 µg/mL of PI (Invitrogen, USA) for 5 min (Iqbal *et al*., 2016). Camptothecin 20 µM and Digitonin 80 µM were used as positive controls for apoptosis and necrosis, respectively, and not treated cells as negative control. The apoptotic cells were visualized in green and necrotic cells in red under an inverted fluorescence microscope (EVOS® FL, Life Technologies, USA).

Detection of intracellular generation of ROS

As described by Nam et al. 2016, conversion of H2DCFDA (emission 515 nm, excitation 492 nm) to highly fluorescent 2′,7′-dichlorofluorescein (DCF) was used to assess total ROS production after experimental treatment. HeLa cell line was seeded in 24-well tissue culture plates with 500 µL/well at a density of 1.5 × 10^5 cells/mL. After overnight incubation, the cells were exposed to 0.4 µmol/L of F127/HYP for 30 min in the absence of light, illuminated for 15 min and then incubated in the absence of light for 30 min. Following, the cells were washed with PBS, fixed with 4% formaldehyde solution for 15 min and treated with 20 µM H2DCFDA solution for 15 min at room temperature protected from light. After washing with PBS, the emitted fluorescence was visualized in an inverted fluorescence microscope (EVOS® FL, Life Technologies, USA).

Assessment of type I and type II photochemical mechanisms

Sodium azide (SA) and D-mannitol (DM) specific scavengers of $^1O_2$ and hydroxyl radicals were respectively used to prevent the ROS formation and to analyze the mechanism of F127/HYP PDT (Cheng *et al*., 2017). The experiment was performed in three groups: IC_{90} value of F127/HYP; IC_{90} value of HYP/F127 and 20 mmol/L SA solution; and IC_{90} value of F127/HYP and 40 mmol/L DM solution. HeLa cells were seeded in 96-well tissue culture plates with 200 µL/well at a density of 2.5 × 10^5 cells/mL and allowed to attach overnight in the incubator. Next, cells were exposed to the different treatments for 30 min in the dark, iluminated for 15 min and incubated in the dark for 30 min. Finally, a MTT assay was performed to determine cell viability.

Cell migration assay

Cell migration after F127/HYP PDT was assessed by Wound-healing assay (Liang *et al*., 2007). HeLa cells were seeded in 6-well tissue culture plates with 2 mL/well at a density of 2×10^5 cells/mL. After 24 hours, the confluent cells were mechanically scratched with a pipet tip (1000 µL) and cell debris was removed by washing with PBS. The treatment was performed with IC_{30} and IC_{50} values of F127/HYP for 30 min in the dark, illuminated for 15 min and incubated again in the dark for 30 min. The cells with DMEM were used as NT. The cell migration into the scratched region was recorded using an inverted microscope EVOS® FL, Life Technologies, USA) at 0, 24, 48, and 72h. Wound closure over time was compared to the initial measurements.

Statistical analysis

At least three independent experiments were performed to express the means ± standard deviation (SD). Significant differences among means were calculated using analysis of variance (ANOVA) followed by Tukey–Kramer multiple comparisons test. All analyzes were performed by GraphPad Prism 6.0 software (GraphPad, San Diego, CA, USA), and P values < 0.05 were considered statistically significant.

RESULTS AND DISCUSSION

F127/HYP-mediated PDT inhibits HeLa tumor cells proliferation but not inhibit HaCaT cells

To evaluate the effects of F127/HYP PDT against cervical adenocarcinoma cells and normal cells, we exposed HeLa and a human immortalized keratinocyte (HaCaT) cell line (control cells), to increasing doses of F127/HYP in the absence of light (Figure 1A) or under light illumination (Figure 1B). In the absence of light (Figure 1A), there was no decrease in cell viability of HeLa and HaCaT exposed to F127/HYP. Also, F127 alone did not showed any cytotoxic effect in the presence and absence of light (Figure 1A and 1B). Similarly, cytotoxicity was observed in HeLa and HaCaT exposed to light in the absence of F127/HYP (NT), indicating that only light exposure at this wavelength causes no effects in the cells (Figure 1B). Damage caused by F127/HYP in the presence of light (Figure 1B) showed selective action in cervical adenocarcinoma cells from the lowest concentration tested (0.40 µmol/L; $p < 0.0001$), as it was not able to significantly reduce HaCaT cell viability at the tested concentrations.

These data indicate that F127/HYP PDT exerted concentration-dependent cytotoxic effects in the cervical adenocarcinoma cell line at low concentrations: IC_{30} (0.90 µmol/L), IC_{50} (1.50 µmol/L) and IC_{90} (2.70 µmol/L). Therefore, our results suggested that low concentrations of F127/HYP micelles, in a short period of incubation and irradiation, can significantly and selectively inhibit the proliferation of cervical adenocarcinoma cells. Other *in vitro* (Xu *et al*., 2019) and *in vivo* (Chen, De Witte, 2000) studies reported HYP low intrinsic toxicity and differential effects in normal versus cancer cells.

The cell growth inhibition induced by F127/HYP PDT was further verified by microscopy. Figure 2 show that the growth of HeLa cells was effectively inhibited with 0.4, 1.8 and 3.2 µmol/L F127/HYP followed by exposure to light. F127/HYP PDT also induced pronounced morphological changes when the cervical adenocarcinoma cell line was exposed to F127/HYP concentrations after illumination. The cells exhibited retraction of cytoplasmic expansion, decreased confluence and detachment from the plate due to cell death.

To further examine the long-term cell proliferation ability and the maintenance of the reproductive capacity to form a large colony or a clone after F127/HYP PDT, a clonogenic cell survival assay was conducted (Franken *et al*., 2006). F127/HYP micelles exerted a reduction of clonogenic potential of HeLa cells after illumination, decreasing the quantity and the size of the circumference of the colonies (Figure 3). HeLa cell's clonogenicity after exposure to F127/HYP and illumination showed a significantly lower number of colonies recovering after 7 and 14 days in comparison to the absence of F127/HYP micelles ($p < 0.0001$). Therefore, F127/HYP PDT treatment exerted long-term concentration-dependent phototoxic effects on

cervical adenocarcinoma cells, which reflects the decrease in long-term cell proliferation. This could indicate a potential ability to prevent recurrence of this type of cancer.

Overall, these results show that F127/HYP-mediated PDT presented a selective dose- and time-dependent cytotoxic effect against cervical adenocarcinoma cells and reduced colony formation at HYP subtoxic doses.

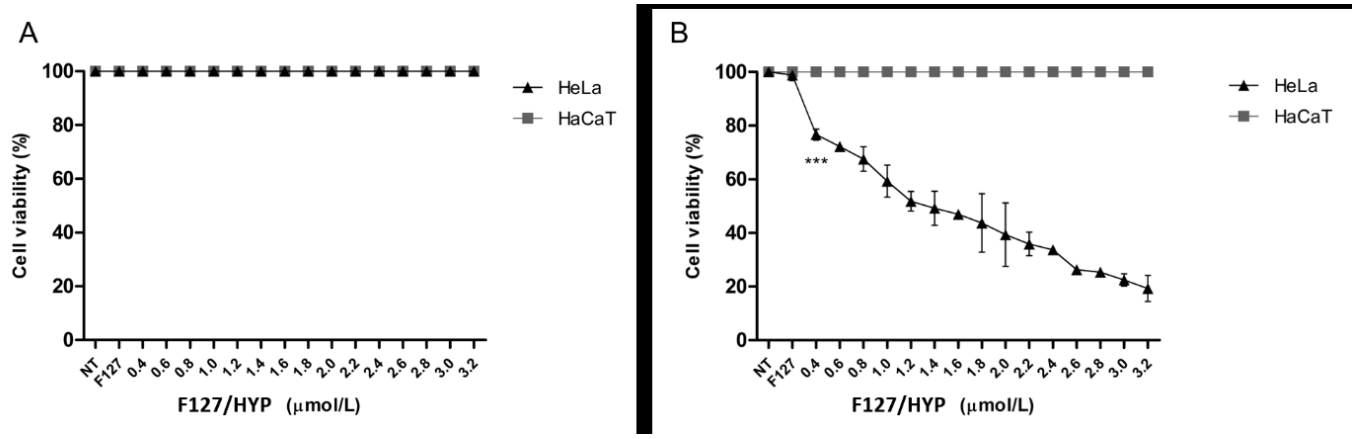

FIGURE 1 - Cytotoxic and phototoxic effects of F127/HYP micelles on HeLa and HaCaT cells, evaluated through MTT assay. (A) Dose-response curves indicating the viability of HeLa and the HaCaT cells not changed following exposure to F127/HYP (0.4–3.2 μmol/L) in the absence of light compared to non-treated (NT) cells. (B) Dose-response curves indicate the significant reduction (***) in the HeLa cells following exposure to F127/HYP (0.4–3.2 μmol/L) in the presence of light compared to NT cells. $P < 0.05$ was considered significant. Each line represents the mean ± SD of three independent experiments conducted in triplicate.

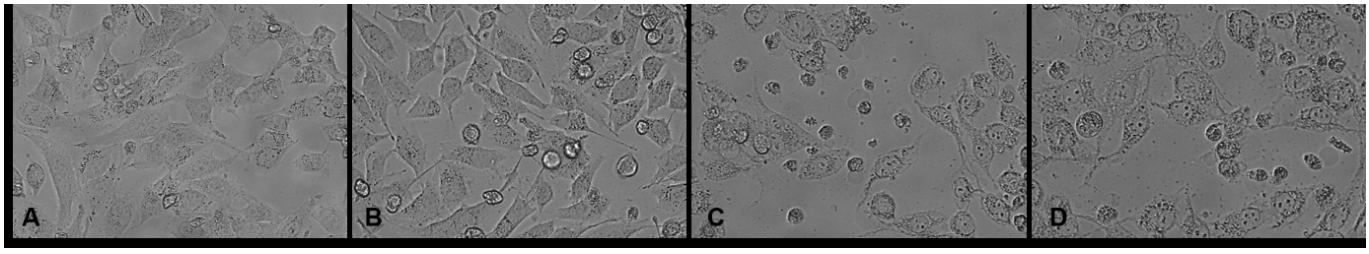

FIGURE 2 - Differential effects on cell morphology induced by F127/HYP in the presence of light. (A) No treated HeLa cells morphology; (B,C,D) HeLa cells morphology after PDT with 0.4 (B), 1.8 (C) and 3.2 (D) μmol/L of HYP/F127. Cell photomicrographs were taken at 20× magnification.

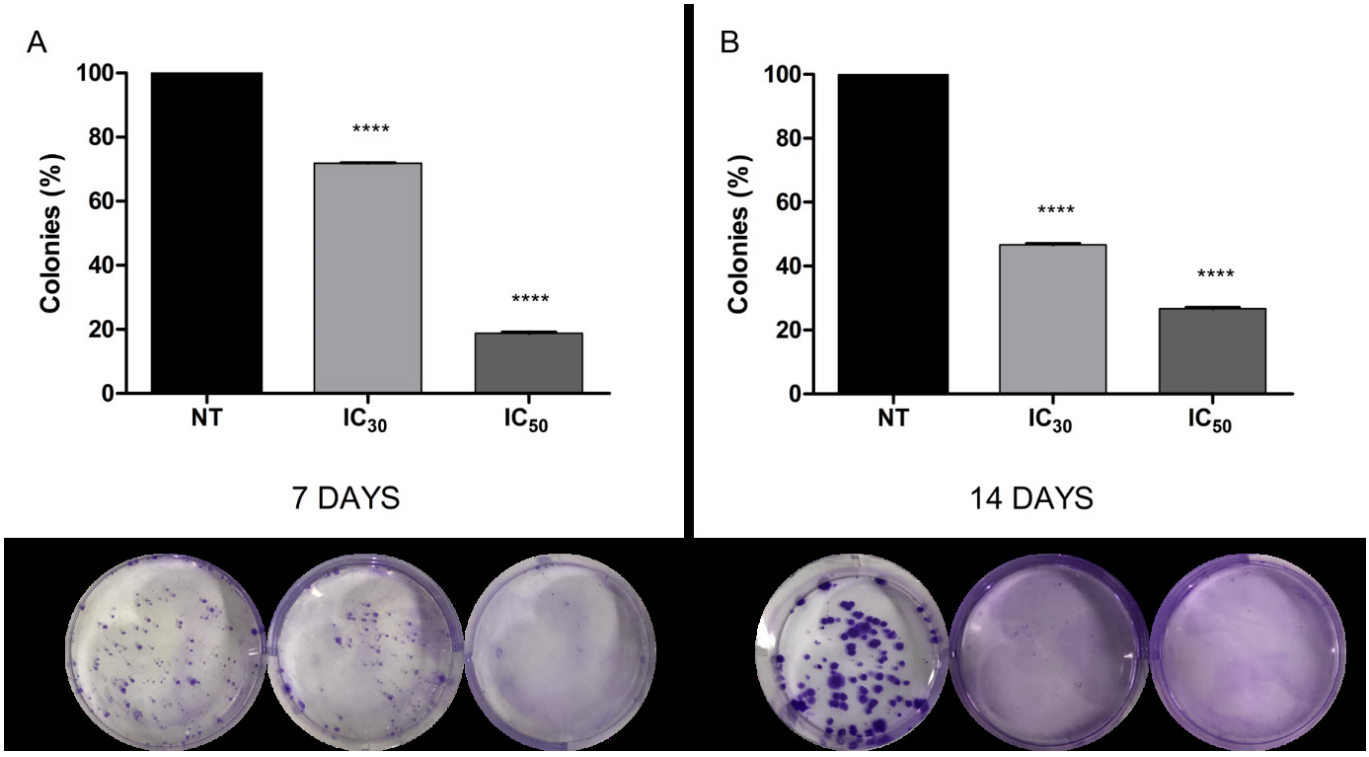

FIGURE 3 - Effect of F127/HYP PDT exposure on the clonogenicity of HeLa cells at (A) 7 and (B) 14 days. The (****) marks statistical significance when comparing treated cell groups (IC_{30} and IC_{50}) with NT. **** $p < 0.0001$.

F127/HYP was actively and selectively internalized by HeLa tumor cells but not by HaCaT cells

The relatively short half-life and low diffusion distances of singlet oxygen require the intracellular localization of the PS drug (Nwahara *et al*., 2021). HYP is naturally fluorescent, so a fluorescence microscopy in the RFP (red) filter was used to evaluate the cellular uptake of F127/HYP at 30 min after micelles incubation. HYP emitted fluorescence at high intensity in HeLa cells treated with 1 µmol/L of F127/HYP micelles (Figure 4C). This fluorescence was observed mainly in their cytoplasm. The same was not observed in HaCaT (Figure 4D).

In face of these findings, we can infer that F127/HYP micelles exhibit a greater ability to permeate the cytoplasmic membrane and to preferentially internalize into the cytoplasm of the HeLa cells rather than in normal cells, indicating its selectivity for cancer cells. Furthermore, the results suggest that the internalization of HYP in HeLa cells was facilitated by F127, which has been previously described as facilitating transport across cytoplasmic membranes or the target binding site (Zhang, Jackson, Burt, 1986; Batrakova, Kabanov, 2008; Imran, Shah, Shafi, 2018).

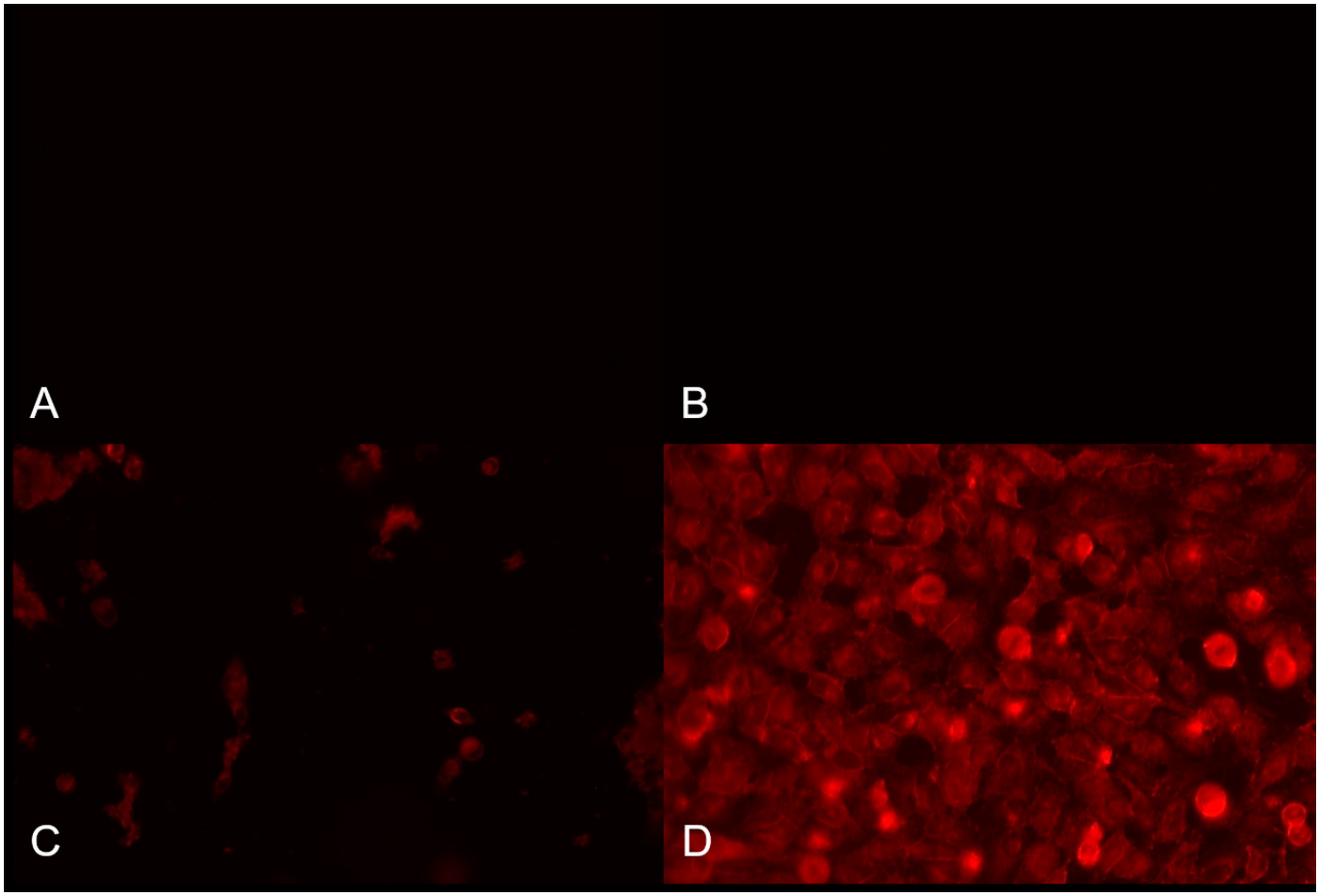

FIGURE 4 - Cellular internalization images were obtained with fluorescent microscopy of (A) HaCaT, (B) untreated HeLa cells, (C) HaCaT and (D) HeLa cells exposed for 30 min to F127/HYP (1 μmol/L); 20x magnification.

F127/HYP leads to HYP distribution in the mitochondria of HeLa cells

Crucial parameters in determining the photocytotoxic activity of HYP are the cell permeability and subcellular localization. The ultimate location of HYP within the cell will determine its apical molecular targets and influence the photocytotoxic activity. Inside cells, $^1O_2$ and the majority of other ROS present extremely short lifetimes and small diffusion radii due to their rapid interaction with biological targets; this interaction leads to a modification of cell functionality and viability (Theodossiou *et al*., 2009). Given the results described above, the subcellular localization of F127/HYP in HeLa cells was examined by specific probes for mitochondria and nucleus. The overlap of the images showed a change of the color in the HYP location in the organelles. Figure 5 shows that F127/HYP treatment at 5 μmol/L led to high fluorescence intensity that coincides with the fluorescence of the mitochondria, which are known to be important cytoplasmic targets for PDT with HYP (Theodossiou *et al*., 2009). Additionally, HeLa cells presented a weak/absent fluorescence of HYP that coincides with the fluorescence of the nucleus, which is in accordance with other studies (Damke *et al*., 2020).

The cellular uptake and subcellular localization of HYP might be affected by its lipophilicity, incubation concentrations and/or interaction with serum lipoproteins (Kascakova *et al*., 2008). In relation to lipophilicity, the subcellular location of the PS is directly associated with its chemical nature. Hydrophobic and hydrophilic PS with more than 2 negative charges in their molecules differs in the ability to diffuse through the plasma membrane and relocate into intracellular membranes. Hydrophobic PS exhibit these abilities whereas hydrophilic PS are captured

by endocytosis because of its high polarity (Nakajima, Kawashima, 2012). Considering these concepts, our results indicate that HYP hydrophobicity was overcome with the Pluronic F127 encapsulation. Pluronics plays a key role in the encapsulation capacity of the PS but also in its delivery, facilitating passive transcellular diffusion across the biomembrane microenvironment via lipophilic domains (Hezaveh *et al*., 2012). Other advantages have been described in addition to stabilizing, protecting and improving the biodistribution of the encapsulated drug (Batrakova, Kabanov, 2008).

Cell death by necrosis or apoptosis after HYP PDT depends mainly on the subcellular localization of HYP (Ho *et al.*, 2009). Generally, photoactive compounds localizing in the mitochondria or the ER promote apoptosis, while photosensitizers that accumulate in the plasma membrane or lysosomes tend to induce cell necrosis (Kessel *et al*., 1997). After identifying that HYP was sublocalized in mitochondria, we evaluated the type of cell death induced after this treatment.

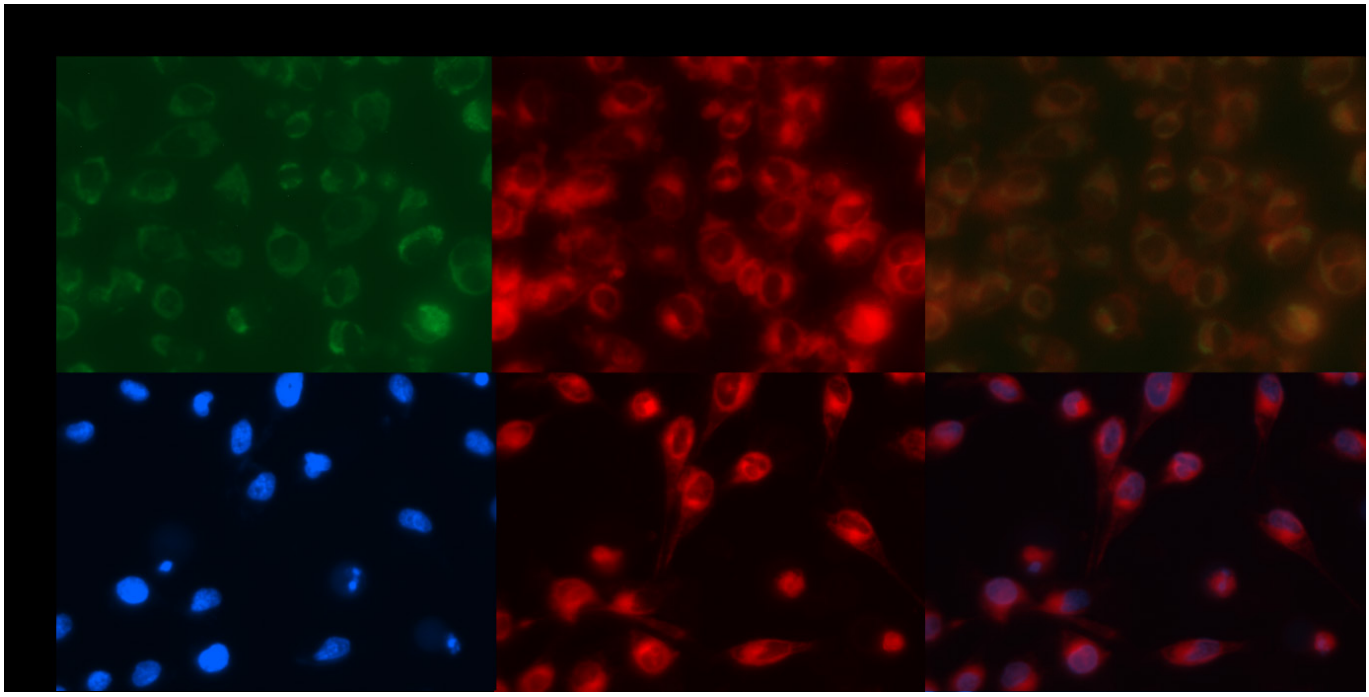

FIGURE 5 - Fluorescent microscopic images of HeLa cells incubated with F127/HYP for 30 min, stained with MitoTracker® (specific probe for mitochondria), and NucBlue® (specific probe for nucleus); 20x magnification.

F127/HYP-mediated PDT induces predominantly cell death by necrosis

To find the type and extent of HeLa cell death, we analyzed whether F127/HYP PDT could induce apoptosis and/or necrosis via an Annexin V-FITC/PI assay using fluorescence microscopy. Annexin-V staining detects the translocation of phosphatidylserine from the inner to the outer cell membrane during early apoptosis (green fluorescence) and PI can enter the cell during necrosis, late-stage apoptosis and dead cells (red fluorescence) (Iqbal *et al*., 2016). As shown in Figure 6, the IC_{50} of F127/HYP can predominantly induce necrosis of HeLa cells. However, the HYP subcellular distribution in the mitochondria of HeLa cells observed by us, suggests a death pathway due to apoptosis. This can be justified because depending on the light dose and concentration of HYP, the strength of the photodynamic process can cause severe damage to

mitochondria, leading to an energy collapse that favors cell death by necrosis or decreases their defenses against this cell death pathway, due to loss of mitochondrial membrane integrity (Theodossiou *et al*., 2009). Still, in certain PDT paradigms, necrosis and not secondary necrosis consequent to apoptotic cell death appears to be the preferential mode of cell death also for photosensitizers originally found in the plasma membrane or subsequently relocalized to other subcellular compartments. This suggests that signaling pathways that orchestrate necrosis rather than apoptosis may exist (Buytaert *et al*., 2007).

Furthermore, our results are consistent with other *in vitro* and *in vivo* studies that showed death by necrosis after HYP PDT (Mikeš *et al*., 2007).

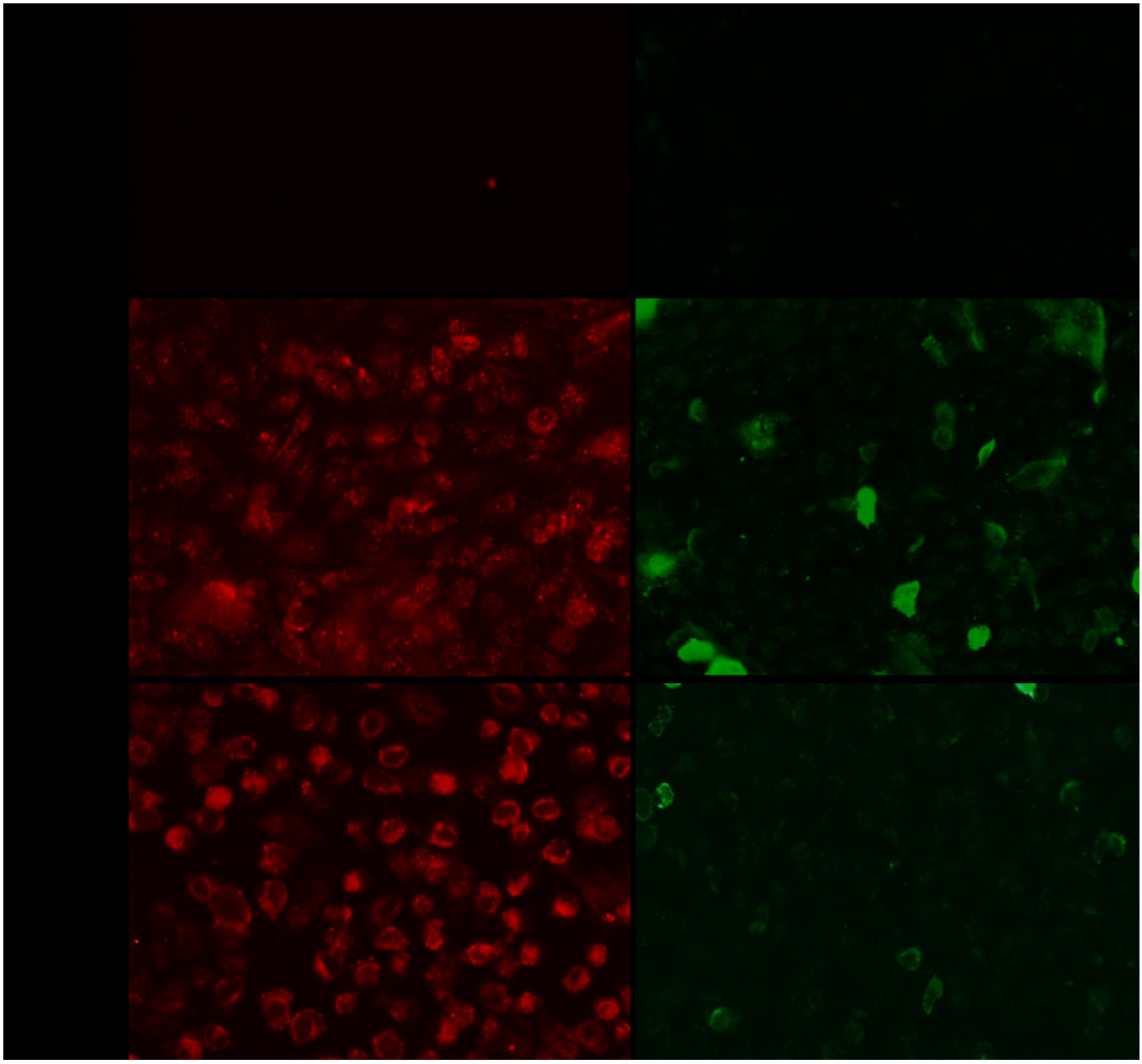

FIGURE 6 – Cell death pathway induced by HYP/F-127 (IC_{50}) in HeLa cells after illumination and stained with annexin V (apoptosis - green fluorescence) and propidium iodide (necrosis - red fluorescence). Camptothecin 20 µM and digitonin 80 µM were positive controls (PC) for apoptosis and necrosis, respectively, and not treated cells as negative control (NC) (20x magnification).

F127/HYP-mediated PDT induces ROS generation mainly by Type II mechanism

Following light excitation, HYP exhibits enhanced *in vitro* cytotoxicity attributed to various ROS. Therefore, we examined the production of total ROS based on an increase in fluorescence that was caused by the conversion of a nonfluorescent dye H2DCFDA to highly fluorescent DCF (Nam *et al*., 2016) after HYP/F127-mediated PDT exposure to 0.4 μmol/L of F127/HYP in the cervical adenocarcinoma cell line. Figure 7 shows the bright-field images and their respective fluorescence images of HeLa cells treated with F127/HYP PDT and untreated cells, that confirm high production of intracellular total ROS via PDT.

Considering that total ROS formation in PDT can occur through two mechanisms (type I and type II) we evaluated these mechanisms. The type I mechanism generates superoxide, hydroxyl radicals, among others. Already in type II mechanism occurs the formation of closely reactive species, known as $^1O_2$ that plays an important role in PDT (Cheng *et al*., 2017). After adding SA and DM during the treatment, ROS originating from PDT would be quenched, resulting in lower PDT action and further increase on cell viability (Cheng *et al*., 2017). Figure 8 shows that the viability of the cell group tested with SA was higher than those treated only with F127/HYP IC_{90} values, suggesting that type II mechanism of PDT is predominant in the cervical adenocarcinoma cells treated with F127/HYP PDT, because the formation of $^1O_2$ was higher than the other ROS. In agreement, other studies highlight evidences that supports a prevalent role for $^1O_2$ in the molecular processes initiated by PDT (Niedre, Patterson, Wilson, 2002) and specifically by HYP (Damke *et al*., 2020).

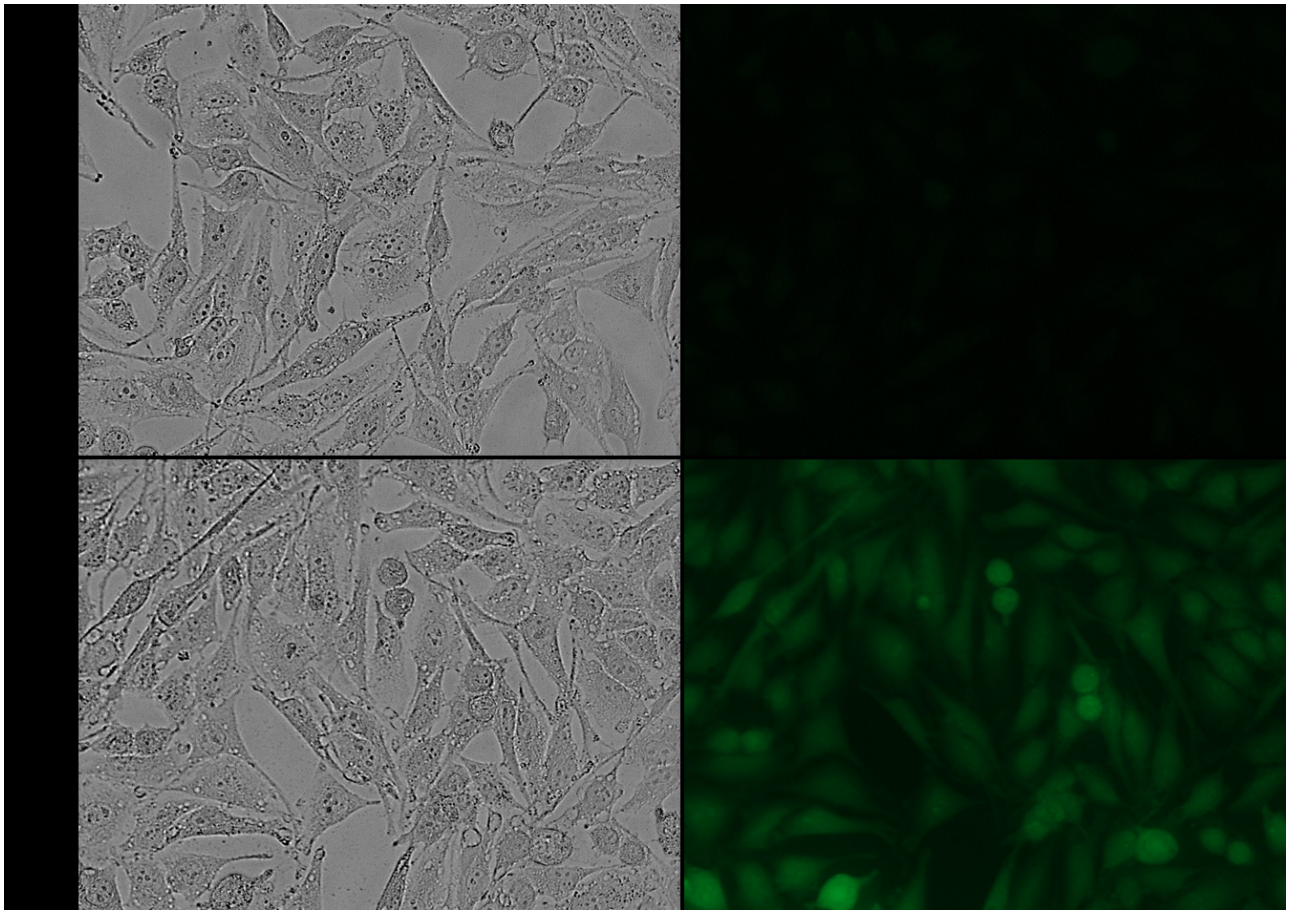

FIGURE 7 - Total intracellular ROS generation: the bright field images and their corresponding fluorescence images of not treated cells (A) and cells treated with 0.4 μmol/L of F127/HYP (B) (20x magnification).

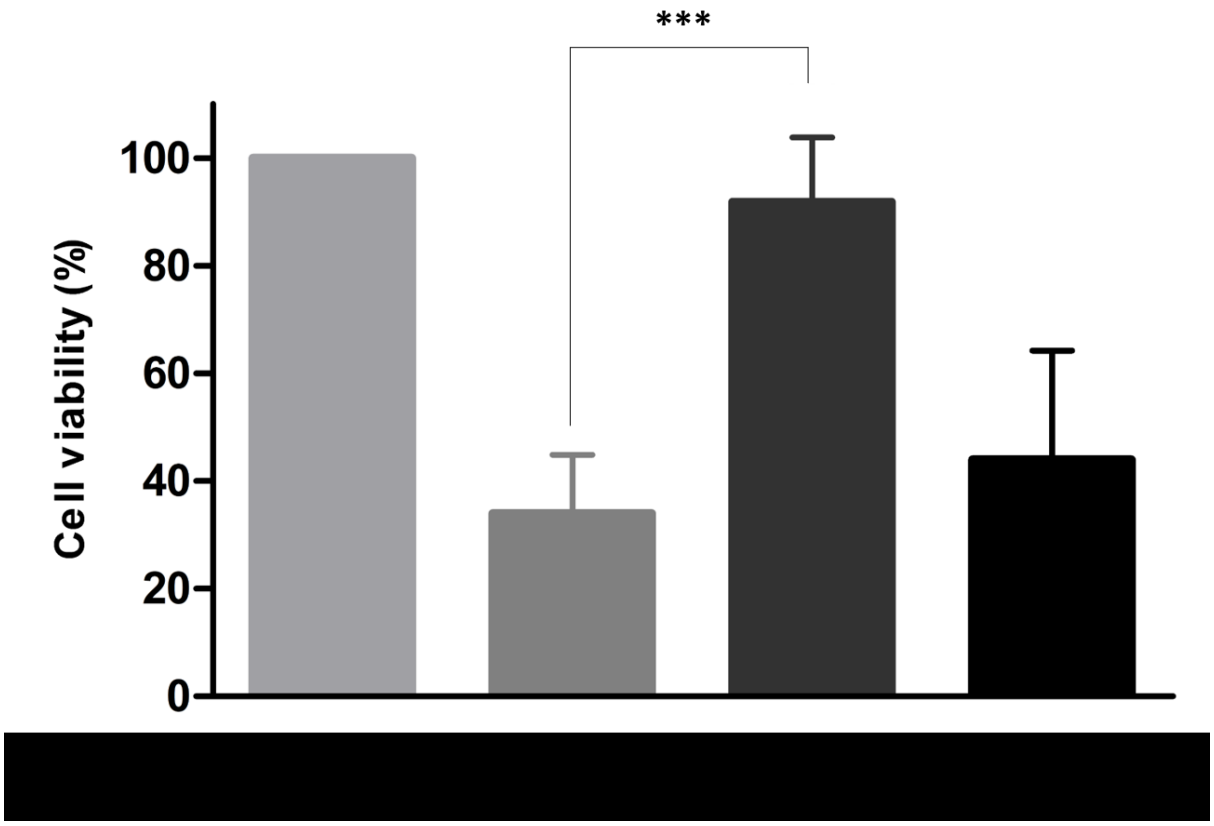

FIGURE 8 - Determination of type I and type II mechanisms of F127/HYP PDT. Each bar represents the mean ± SD of three independent experiments conducted in triplicate, *** $p < 0.001$.

F127/HYP-mediated PDT inhibits cell migration

To examine the effect of F127/HYP micelles on cervical adenocarcinoma cell migration, a wound-healing assay was performed. As shown in Figure 9, F127/HYP (IC_{30} and IC_{50}) presented an expressive inhibition of the HeLa cell's basal migratory ability at all times tested ($p < 0.001$) after illumination. Total wound closure was only observed in not treated cells within 72 h, which were able to migrate and promote full cell confluence, highlighting the effect of the F127/HYP micelles in avoiding the migration and invasion of adenocarcinoma cells, possibly by decreasing their ability to form metastases.

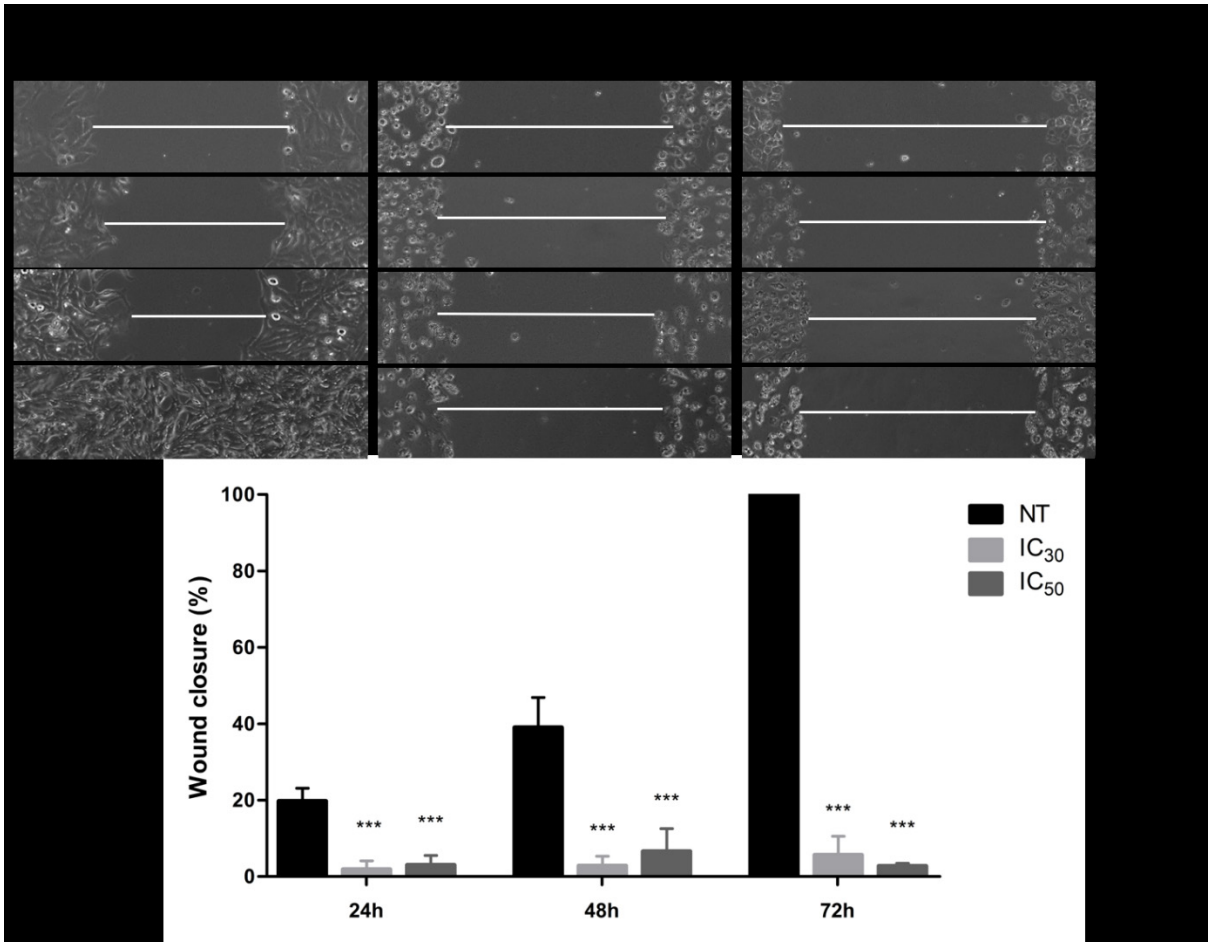

FIGURE 9 - Cell migration analysis by the wound-healing assay. (A) HeLa cells after scratching in the absence (NT) and presence of F127/HYP micelles (IC_{30} and IC_{50}) and after illumination (20x magnification). (B) Percentage of wound closure after 24, 48 and 72h compared to the wound measurement at the initial time. Data are shown as the means ± SD of three independent experiments in triplicate. ***$p < 0.001$.

CONCLUSION

As far as we know, this study was the first to investigate the efficacy of HYP encapsulated on Pluronic F127 (F127/HYP) PDT against human cervical adenocarcinoma-derived cell line HeLa (HPV-18 positive). We showed that F127/HYP micelles presented effective and selective time- and dose-dependent phototoxic effects against ECA cells and no effects against non-tumor cells (HaCaT). Additionally, F127/HYP micelles exhibited selective internalization in the cervical adenocarcinoma cell line, indicating their potential to permeate the membrane of these cells. Moreover, F127/HYP micelles accumulated in mitochondria organelle, resulting in photodynamic cell death by necrosis. F127/HYP micelles were able to inhibit the formation of cellular colonies, suggesting an ability to avoid the recurrence of ECA. Finally, we also showed that F127/HYP PDT inhibited the migration and invasion of HeLa cells, showing its potential in preventing the migration of tumor cells, decreasing the chance of metastases. Our results indicate a potentially useful role of F127 micelles as a platform for HYP delivery to more specifically and effectively treat cervical adenocarcinomas through PDT, suggesting they are worthy for *in vivo* preclinical evaluations**.**

ACKNOWLEDGMENTS

This work was supported by Conselho Nacional de Desenvolvimento Científico e Tecnológico (CNPq; grants

304037/2019-2 and 409382/2018-3) and Coordenação de Aperfeiçoamento de Pessoal de Nível Superior /CAPES for the scholarships.

REFERENCES

Agostinis P, Berg K, Cengel KA, Foster TH, Girotti AW, Gollnick SO, et al. Photodynamic therapy of cancer: An update. CA Cancer J Clin. 2011;61(4):250–281.

Batrakova E V, Kabanov A V. Pluronic block copolymers: evolution of drug delivery concept from inert nanocarriers to biological response modifiers. J Control Release. 2008;130(2):98–106.

Buytaert E, Dewaele M, Agostinis P. Molecular effectors of multiple cell death pathways initiated by photodynamic therapy. Biochim Biophys Acta Rev Cancer. 2007;1776(1):86–107.

Chen B, De Witte PA. Photodynamic therapy efficacy and tissue distribution of hypericin in a mouse P388 lymphoma tumor model. Cancer Lett. 2000;150(1):111–117.

Cheng J, Li W, Tan G, Wang Z, Li S, Jin Y. Synthesis and in vitro photodynamic therapy of chlorin derivative 13 1-ortho-trifluoromethyl-phenylhydrazone modified pyropheophorbide-a. Biomed Pharmacother. 2017;87:263–273.

Chung P-S, Saxton RE, Paiva MB, Rhee C-K, Soudant J, Mathey A, et al. Hypericin uptake in rabbits and nude mice transplanted with human squamous cell carcinomas: study of a new sensitizer for laser phototherapy. Laryngoscope. 1994;104(12):1471-1476.

Damke GMZF, Damke E, de Souza Bonfim-Mendonça P, Ratti BA, de Freitas Meirelles LE, da Silva VRS, et al. Selective photodynamic effects on cervical cancer cells provided by P123 Pluronic®-based nanoparticles modulating hypericin delivery. Life Sci. 2020;255:117858255.

Falk H, Schoppel G. On the synthesis of hypericin by oxidative trimethylemodin anthrone and emodin anthrone dimerization: Isohypericin. Monatshefte Chemie Chem Mon. 1992;123(10):931–938.

Franken NAP, Rodermond HM, Stap J, Haveman J, van Bree C. Clonogenic assay of cells in vitro. Nat Protoc. 2006;1(5):2315–2319.

Fuchs J, Thiele J. The role of oxygen in cutaneous photodynamic therapy. Free Radicals Biol Med. 1998;24(5):835–847.

Gonçalves RS, Rabello BR, César GB, Pereira PCS, Ribeiro MAS, Meurer EC, et al. An Efficient Multigram Synthesis of Hypericin Improved by a Low Power LED Based Photoreactor. Org Process Res Dev. 2017;21(12):2025–2031.

Gregoriou Y, Gregoriou G, Yilmaz V, Kapnisis K, Prokopi M, Anayiotos A, et al. Resveratrol loaded polymeric micelles for theranostic targeting of breast cancer cells. Nanotheranostics. 2021;5(1):113.

Hezaveh S, Samanta S, De Nicola A, Milano G, Roccatano D. Understanding the interaction of block copolymers with DMPC lipid bilayer using coarse-grained molecular dynamics simulations. J Phys Chem B. 2012;116(49):14333–14345.

Ho YF, Wu MH, Cheng BH, Chen YW, Shih MC. Lipid-mediated preferential localization of hypericin in lipid membranes. Biochim Biophys Acta Biomembr. 2009;1788(6):1287–1295.

Hudson JB, Lopez-Bazzocchi I, Towers GHN. Antiviral activities of hypericin. Antiviral Res. 1991;15(2):101–12.

Imran M, Shah MR, Shafi U. Amphiphilic block copolymers–based micelles for drug delivery. Des Dev New Nanocarriers. 2018;2018:365–400.

Iqbal B, Ghildiyal A, Sahabjada, Singh S, Arshad M, Mahdi AA, et al. Antiproliferative and apoptotic effect of curcumin and TRAIL (TNF Related Apoptosis inducing Ligand) in chronic myeloid leukaemic cells. J Clin Diagn Res. 2016;10(4):XC01–5.

Karioti A, Bilia AR. Hypericins as Potential Leads for New Therapeutics. Int J Mol Sci. 2010;11(2):562.

Kascakova S, Nadova Z, Mateasik A, Mikes J, Huntosova V, Refregiers M, et al. High level of low-density lipoprotein receptors enhance hypericin uptake by U-87 MG cells in the presence of LDL. Photochem Photobiol. 2008;84(1):120–127.

Kessel D, Luo Y, Deng Y, Chang CK. The role of subcellular localization in initiation of apoptosis by photodynamic therapy. Photochem Photobiol. 1997;65(3):422–426.

Kubin A, Loew HG, Burner U, Jessner G, Kolbabek H, Wierrani F. How to make hypericin water-soluble. Pharmazie. 2008;63:263–269.

Kumar P, Nagarajan A, Uchil PD. Analysis of Cell Viability by the MTT Assay. Cold Spring Harb Protoc. 2018;2018(6).

Kurman R, Carcangiu M, Herrington C, Young R. WHO Classification of Tumours of Female Reproductive Organs. 4th ed. Kurman R, Carcangiu M, Herrington C, Young R, editors. Lyon: IARC; 2014.

Liang CC, Park AY, Guan JL. In vitro scratch assay: a convenient and inexpensive method for analysis of cell migration in vitro. Nat Protoc. 2007;2(2):329–333.

Loureiro J, Oliva E. The spectrum of cervical glandular neoplasia and issues in differential diagnosis. Arch Pathol Lab Med. 2014;138(4):453–483.

Mikeš J, Kleban J, Sačková V, Horváth V, Jamborová E, Vaculová A, et al. Necrosis predominates in the cell death of human colon adenocarcinoma HT-29 cells treated under variable conditions of photodynamic therapy with hypericin. Photochem Photobiol Sci. 2007;6(7):758–766.

Nakajima N, Kawashima N. A basic study on Hypericin-PDT *in vitro*. Photodiag Photodyn Ther. 2012;9(3):196–203.

Nam G, Rangasamy S, Ju H, Samson AAS, Song JM. Cell death mechanistic study of photodynamic therapy against breast cancer cells utilizing liposomal delivery of 5,10,15,20-tetrakis(benzo[b]thiophene) porphyrin. J Photochem Photobiol B. 2016;166:116–125.

Niedre M, Patterson MS, Wilson BC. Direct near-infrared luminescence detection of singlet oxygen generated by photodynamic therapy in cells in vitro and tissues in vivo. Photochem Photobiol. 2002;75(4):382–391.

Nwahara N, Abrahams G, Prinsloo E, Nyokong T. Folic acid-modified phthalocyanine-nanozyme loaded liposomes for targeted photodynamic therapy. Photodiagnosis Photodyn. Ther. 2021;36.

Ochsner M. Photophysical and photobiological processes in the photodynamic therapy of tumours. J Photochem Photobiol B. 1997;39(1):1–18.

Paik ES, Lim MC, Kim MH, Kim YH, Song ES, Seong SJ, et al. Prognostic Model for Survival and Recurrence in Patients with Early-Stage Cervical Cancer: A Korean Gynecologic Oncology Group Study (KGOG 1028). Cancer Res Treat. 2020;52(1):320–333.

Robertson CA, Evans DH, Abrahamse H. Photodynamic therapy (PDT): A short review on cellular mechanisms and cancer research applications for PDT. J Photochem Photobiol B. 2009;96(1):1–8.

de Souza MVF, Shinobu-Mesquita C, Meirelles LE, Mari N, César G, Gonçalves R, et al. Effects of hypericin encapsulated on Pluronic F127 photodynamic therapy against triple negative breast cancer. Asian Pac J Cancer Prev. 2022;23(5):1741–1751.

Stolnicu S, Hoang L, Soslow RA. Recent advances in invasive adenocarcinoma of the cervix. Virchows Arch. 2019;475(5):537-549.

Sung H, Ferlay J, Siegel RL, Laversanne M, Soerjomataram I, Jemal A, et al. Global Cancer Statistics 2020: GLOBOCAN Estimates of Incidence and Mortality Worldwide for 36 Cancers in 185 Countries. CA Cancer J Clin. 2021;71(3):209–249.

Tatischeff I, Alfsen A. A New Biological Strategy for Drug Delivery: Eucaryotic Cell-Derived Nanovesicles. J Biomater Nanobiotechnol. 2011;2(5):494–499.

Theodossiou TA, Hothersall JS, De Witte PA, Pantos A, Agostinis P. The multifaceted photocytotoxic profile of hypericin. Mol Pharm. 2009;6(6):1775–1789.

Xu L, Zhang X, Cheng W, Wang Y, Yi K, Wang Z, et al. Hypericin-photodynamic therapy inhibits the growth of adult T-cell leukemia cells through induction of apoptosis and suppression of viral transcription. Retrovirol. 2019;16(1):1–13.

Yokoi E, Mabuchi S, Takahashi R, Matsumoto Y, Kuroda H, Kozasa K, et al. Impact of histological subtype on survival in patients with locally advanced cervical cancer that were treated with definitive radiotherapy: adenocarcinoma/adenosquamous carcinoma versus squamous cell carcinoma. J Gynecol Oncol. 2017;28(2):e19.

Zhang X, Jackson JK, Burt HM. Development of amphiphilic diblock copolymers as micellar carriers of taxol. Int J Pharm. 1996;132(1–2):195–206.

Received for publication on 01st July 2022
Accepted for publication on 25th November 2022